Volume 10, Issue 2, 2020, 5117 - 5121 **ISSN 2069-5837**

Biointerface Research in Applied Chemistry

www.BiointerfaceResearch.com

https://doi.org/10.33263/BRIAC102.117121

Original Review Article **Open Access Journal**

Received: 05.01.2020 / Revised: 25.01.2020 / Accepted: 26.01.2020 / Published on-line: 28.01.2020

The search for peptide deformylase inhibitor from Indonesian Medicinal Plant Database: an *in-silico* investigation

Muhammad Arba [1,*], Akbar Reformasi Pangan [1], Arry Yanuar [2]

[1]Faculty of Pharmacy, Universitas Halu Oleo, Kendari, Indonesia, 93232
[2]Faculty of Pharmacy, Universitas Indonesia, Depok, Indonesia, 16424

*corresponding author e-mail address: ***muh.arba@uho.ac.id*** | Scopus ID 57155296400

ABSTRACT

The peptide deformylase protein (PDF) has emerged as a promising target for the discovery of novel antibiotics with a novel mechanism of action. The current investigation was aimed at identifying potential inhibitor of PDF by using structure-based pharmacophore modelling. The pharmacophore hypothesis consisted of one hydrophobic, one negative ionizable, and one hydrogen bond donor features which were built using the structure of cognate ligand of PDF (BB2). Further, the pharmacophore model was validated and used to screen hit molecule against Indonesian Medicinal Plant Database and retrieved 32 hit molecules. All hit molecules were docked to PDF and four best molecules were subjected for 50-ns molecular dynamics (MD) simulation. MD simulation confirmed the docked poses of ligand as indicated by the RMSD and RMSF values. Prediction of affinities employing Molecular Mechanics Poisson-Boltzmann Surface Area (MM-PBSA) method revealed that quercetin 3-(6''-malonylneohesperidoside) had a comparable affinity with that of BB2, which indicated its potential as a novel herbal-based PDF inhibitor.

Keywords: *pharmacophore modeling; peptide deformylase protein (PDF); molecular dynamics simulation; virtual screening; MM-PBSA.*

1. INTRODUCTION

Today's era has witnessed a rising incidence of resistance to the existing medicines of human infections. Several examples include Staphylococcus aureus resistance against methicillin, Enterococcus resistance against vancomycin, multidrug-resistant *Mycobacterium tuberculosis,* and Streptococcus pneumoniae resistance against penicillin [1, 2]. The overuse of antibiotics contributes to the emerging resistance, and as a result, infectious diseases become one of the main causes of death worldwide. Therefore, there is a pressing need for developing new antimicrobial agent which target drug-resistant pathogens. In this issue, novel target which proposes a new mechanism of action will be highly desired. Peptide deformylase (PDF) (EC 3.5.1.31), a clinically unexploited antibacterial target, is a bacterial metalloenzyme which is essential for developing mature protein of bacterial. PDF is responsible for removing N-formyl group of the terminal N-formylmethionine residue of the newly synthesized polypeptide using a ferrous ion (Fe^{2+}) [3, 4]. It is the necessary step of bacterial protein synthesis but is not required in mammalian cell survival [5, 6]. Therefore, PDF has emerged as one of the promising therapeutic targets of antibiotic chemotherapy [7] and there is no currently PDF inhibitor being used clinically.

The first discovered PDF inhibitor occurring naturally, Actinonin, exhibited moderate activity against Gram-positive and Gram-negative bacteria but suffering low structural stability and quick clearance. Another PDF inhibitor, LBM415, has progressed into clinical trial phase I for respiratory infection-related activity but having a safety issue. While lanopepden (GSK1322322) entered clinical trial phase II with effective antibacterial activity against skin pathogens, however, issue on reactive metabolites was emerged [1, 8, 9]. On the other hand, the medicinal plant has been recognized for decades as a source of human medicine. There is plenty of example in which natural resources contribute for chemotherapeutic agent. The present study aims to explore the potency of Indonesian medicinal plant for finding PDF inhibitor by performing pharmacophore based virtual screening. Virtual screening method has long played important roles in the discovery of bioactive molecules, particularly for its advantageous time and cost efficiency. In this study, a pharmacophore model was developed and employed for screening of PDF inhibitor. Molecular docking was performed to reveal the binding mode of hit molecules, while molecular dynamics (MD) simulation in conjunction with MM-PBSA calculation was conducted to explore the structural and energetics aspect of molecules in complex with PDF.

2. MATERIALS AND METHODS

2.1. Pharmacophore modelling and database screening.

The ligand-bound crystal structure was imported from the Research Collaboratory for Structural Bioinformatics (RCSB) Protein Data Bank with the PDB ID 1LRU [10]. The pharmacophore model was built based on the crystal structure by employing LigandScout Advanced 4.3 software [11]. Model validation was conducted against 161 actives and 5730 decoys retrieved from the Directory of Useful Decoys-Enhanced (DUD-E) [12]. The validated model was then used for screening against

internal Indonesian medicinal plant database which contained 1379 molecules.

2.2. Molecular docking and molecular dynamics studies.

Molecular docking was a computational tool to predict the binding orientation of hit molecules in the active site of PDF. It involves two steps, i.e. predicting the binding modes and estimation of binding energy of ligand-protein complex. Each hit molecule resulted from pharmacophore screening was subjected to molecular docking in the active site of PDF by using iDock software [13]. The same PDF structure which was complexed with Actinonin (BB2) was used. The protein was firstly prepared by adding polar hydrogen and assigning Kollman charges using AutoDockTools 1.5.6 [14]. The setting of the grid box for docking follows the coordinates of BB2 with a size of 22.5 × 22.5 × 22.5 Å in XYZ dimensions. Docking validation was achieved by redocking the native ligand (BB2) into PDF. Visualization of docked poses was performed by using Discovery Studio Visualizer 2016. The four top-docked molecules were submitted for molecular dynamics study.

Molecular dynamics (MD) simulation was conducted for 50 ns with periodic boundary condition by using Amber16 software. The AMBER ff14SB force field [15] was used to process protein, while GAFF force field [16] and AM1-BCC [17] were used to treat ligands. Each complex was immersed in a truncated octahedron TIP3P water box with a 10 Å radius. Counterions were added to neutralized complex. All system preparation, minimization, heating, equilibration, and production steps follow our previous procedure [18]. The root means square deviation (RMSD) values were taken for assessing complex stability during MD simulation. The binding energy of ligand in complex with PDF was calculated employing the Molecular Mechanics-Poisson Boltzmann solvent accessible surface area (MM-PBSA) method [19–21] as implemented in MMPBSA.py module of AMBER16 [23]. Trajectories from 30-50 ns MD simulation was used for the calculation.

3. RESULTS

The pharmacophore modeling was applied to develop a model which is then used to screen molecules in the database. Several models were generated, and one model was chosen which satisfy the validation criteria. It composed of one hydrophobic, one negative ionizable, and one hydrogen bond donor. Figure 1 displays the pharmacophore model chosen.

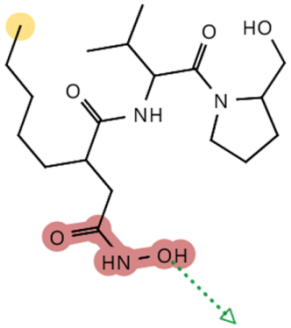

Figure 1. 3D pharmacophore model composed of one hydrophobic (yellow sphere), one negative ionizable (red line), and one hydrogen bond donor (green dotted lines) features.

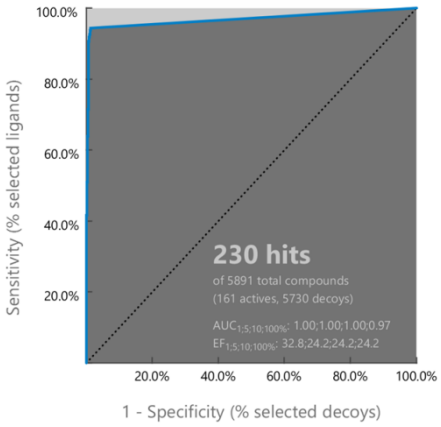

Figure 2. The Area Under Curve (AUC) of Receiver Operating Characteristic (ROC) curve.

Validation of the model against 161 actives and 5730 decoys generated the value of Area Under Curve (AUC) of Receiver Operating Characteristic (ROC) of 0.97. Figure 2 shows Area Under Curve (AUC) of Receiver Operating Characteristic (ROC) curve.

In addition, the score of Goodness Hit was 0.72, which indicated that the model was able to differentiate the actives from the decoy molecules. Further, screening against Indonesian Herbal database (1379 molecules) employing the validated pharmacophore model retrieved 32 hit molecules. While molecular docking on 32 hits to PDF resulted in conformations and binding energies in the interval of −5.14 to −9.71 kcal/mol. The binding energies of hit molecules were comparable to that of BB2 (−7.32 kcal/mol) with RMSD value of 1.597 Å, which indicates that the docking protocol employed in the present study was valid [14]. The key hydrogen bonds (Hbonds) of BB2 in the X-ray experiment were reproduced in a docked pose, i.e. those with Ile44, Gln50, and Gly89[10]. Figure 3 shows the superimposed BB2 conformations of both experimental and docked experiments.

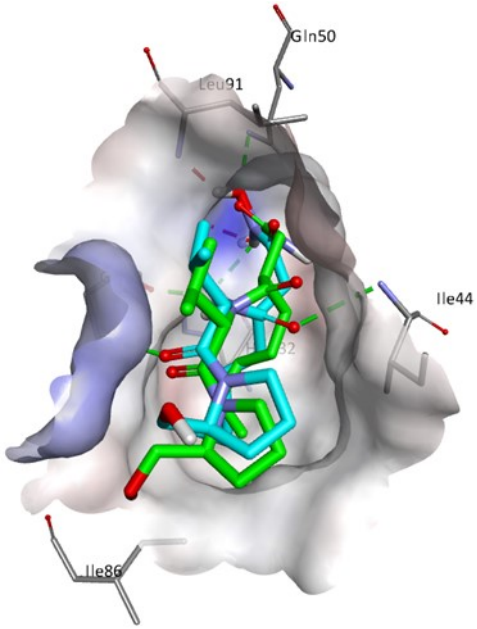

Figure 3. The superimposed BB2 conformations of both experimental (green) and docked (blue) experiments.

Based on the binding energies and conformations, four best docked hit molecules were selected. They were Miquelianin (E=−9.71 kcal/mol), Quercetin 3-(6"-malonylneohesperidoside)

(E=−9.21 kcal/mol), Gibberellin A23 (E=−9.00 kcal/mol), and Quercetin 4'-glucuronide (E=−8.91 kcal/mol). Figure 4 shows the chemical structures of the four best docked hit molecules.

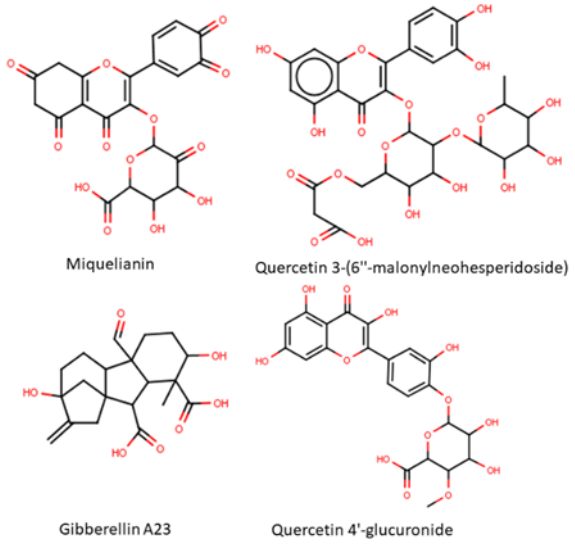

Figure 4. The chemical structures of four best docked hit molecules.

Binding of hit molecules occurred through crucial amino acid residues of PDF. Hbond interactions were made between Miquelianin with Ile44, Arg97, and His132. The Zinc atom of PDF was also interacted with ligand. The amino acid residues of Ile44 and Arg97 was also established Hbonds with Quercetin 3-(6''-malonylneohesperidoside), with additional Hbonds with Glu42 and Pro94. While Gibberellin A23 made Hbonds with Gly89 and Glu133, Quercetin 4'-glucuronide interacts with Glu41, Ile44, Glu95, and His132. Figure 5 displays the binding modes of each hit molecules into the active site of PDF.

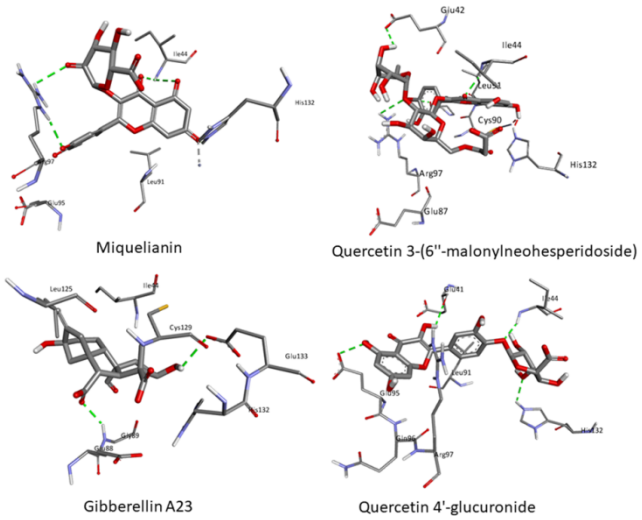

Figure 5. The binding orientation of Miquelianin, Quercetin 3-(6''-malonylneohesperidoside), Gibberellin A23, and Quercetin 4'-glucuronide in the active site of PDF.

3.1. Molecular dynamics simulations.

50 ns MD simulation was performed to examine the structure and energetics of four best docked hit molecules in complex with PDF. System equilibration was verified using RMSD values, which show that each complex reached equilibrium after 17 ns (Figure 6). Complex of Miquelianin, Quercetin 3-(6''-malonylneohesperidoside), and Gibberellin A23 show lower RMSD values than that of BB2 (red) as indicated in both RMSD values of main protein and those of ligand atoms.

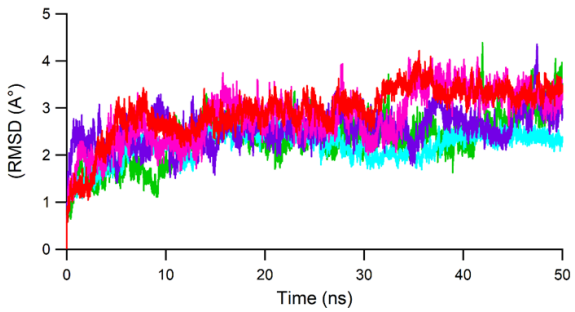

Figure 6. RMSD value of protein backbone atoms (a) and RMSD value of ligand atoms (b) along 50 ns MD run; in which BB2 assigned as (red), Miquelianin (green), Quercetin 3-(6''-malonylneohesperidoside) (blue), Gibberellin A23 (purple), and Quercetin 4'-glucuronide (pink).

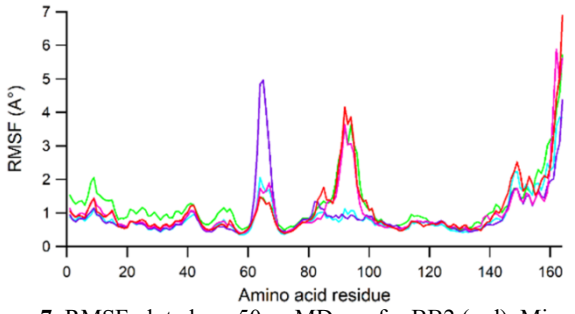

Figure 7. RMSF plot along 50 ns MD run for BB2 (red), Miquelianin (green), Quercetin 3-(6''-malonylneohesperidoside) (blue), Gibberellin A23 (purple), and Quercetin 4'-glucuronide (pink).

While, fluctuation on PDF amino acid residues along MD run were recorded in root mean square fluctuation (RMSF) plot (Figure 7). The RMSF plot shows that all complex fluctuated in a similar pattern in all regions of PDF, which indicate the similar binding modes of molecules. Peaks of Asn65 and Ser92 was observed higher than those of other regions, which associated with the loop regions of PDF. While, Leu164 was also high due to the ends of the protein chain. Other regions including those involved in hydrogen bond interactions showed rigidity, which indicated that the ligand binding induced stability over the protein fluctuation.

In addition, hydrogen bond (Hbond) occupancies was also monitored during MD run. The Hbonds interactions showed varied occupancies during MD run. For example, the Hbonds of Quercetin 3-(6''-malonylneohesperidoside) with Ile93 and His132 showed high occupancies of 84.25% and 64.83%, respectively. The Hbond with Tyr813 showed very low occupancy which was only 0.56%. In the binding of Quercetin 4'-glucuronide, several Hbonds with Gln96, Glu87, Glu95, and Arg153 were found with occupancies ranging from 38.18% to 15.96%. Whereas, Hbonds between Gibberellin A23 and Glu87 and His132 had 30.58% and 10.94% occupancies. The Miquelianin showed very low Hbond occupancies in the range of 0.3 and 3.23% with Glu87, Gly89, Arg97, and Ile44. Table 1 shows the Hbond occupancies along MD run.

3.2. Free binding energy calculations.

Table 2 shows the binding free energy (in kcal/mol) of hit molecule calculated by MM-PBSA method. Quercetin 3-(6''-malonylneohesperidoside) had the lowest predicted binding free energy (ΔE_{PBTOT}=−133.34±20.35 kcal/mol), which was comparable with that of BB2 (ΔE_{PBTOT}=−138.74±21.92kcal/mol). The hit molecule Quercetin 4'-glucuronide scored second best binding free energy (ΔE_{PBTOT}=−109.30±18.63 kcal/mol), followed by the molecule hits Gibberellin A23 (ΔE_{PBTOT}=−79.41±18.67

kcal/mol), and Miquelianin (ΔE_{PBTOT}=−21.96±2.12 kcal/mol). Binding free energy calculation revealed that the binding of ligand was governed by van der Waals (ΔE_{VDW}) energies. Elecrostatic energies (ΔE_{ELE}) was also supporting the binding of ligand except for Quercetin 3-(6"-malonylneohesperidoside). However, it compensated the positive electrostatic energy by negative polar contribution of solvation energy (ΔE_{PBCAL}).

Table 1. The hydrogen bond occupancy each ligand-PDT complex.

Ligand	Acceptor	Donor	Occupancy (%)	Distance (Å)	Angle
Miquelianin	GLU_87@O	LIG@H44: LIG@O30	3.23	2.83	152.4276
	LIG@O21	GLY_89@H: GLY_89@N	2.7	2.91	155.4855
	LIG@O19	ARG_97@HE: ARG_97@NE	1.1	2.90	145.7795
	LIG@O17	ILE_44@H: ILE_44@N	0.3	2.91	152.3937
Quercetin 3-(6''-malonylneohesperidoside)	ILE_93@O	LIG@H26: LIG@O25	84.25	2.73	161.02
	LIG@O76	HIE_132@HE2: HIE_132@NE2	64.83	2.85	155.85
	GLU_42@O	LIG@H66: LIG@O65	23.37	2.73	160.94
	GLN_96@O	LIG@H72: LIG@O71	17.64	2.80	144.19
	GLU_41@O	LIG@H66: LIG@O65	13.3	2.74	164.21
Gibberellin A23	GLU_87@O	LIG@H41: LIG@O40	30.58	2.73	164.22
	HIE_132@ND1	LIG@H41: LIG@O40	24.1	2.86	158.65
	GLU_87@OE1	LIG@H48: LIG@O47	10.94	2.69	164.19
Quercetin 4'-glucuronide	GLN_96@OE1	LIG@H30: LIG@O29	38.18	2.66	156.49
	GLU_87@OE1	LIG@H24: LIG@O23	21.99	2.64	163.84
	GLU_87@OE2	LIG@H24: LIG@O23	19.89	2.64	164.11
	GLU_95@OE1	LIG@H48: LIG@O47	16.02	2.69	163.97
	LIG@O51	ARG_153@HH21: ARG_153@NH2	15.96	2.81	157.31

Table 2. The binding free energy and their individual energy contributions.

Ligand	ΔE_{ELE} (kcal/mol)	ΔE_{VDW} (kcal/mol)	ΔE_{PBCAL} (kcal/mol)	ΔE_{PBSUR} (kcal/mol)	ΔE_{PBTOT} (kcal/mol)
BB2	−66.61±6.11	−144.26±20.69	75.65±8.87	−3.53±0.26	−138.74±21.92
Miquelianin	−0.68±1.92	−29.75±2.16	11.09±2.20	−2.61±0.12	−21.96±2.12
Quercetin 3-(6''-malonylneohesperidoside)	77.30±19.48	−179.66±19.27	−26.38±18.91	−4.60±0.15	−133.34±20.35
Gibberellin A23	−26.96±11.58	−111.48±16.61	41.70±9.53	−2.90±0.14	−79.41±18.67
Quercetin 4'-glucuronide	−102.96±33.08	−118.84±18.32	115.97±30.02	−3.47±0.19	−109.30±18.63

4. CONCLUSIONS

Pharmacophore modeling, molecular docking, MD simulation, and MM-PBSA calculation were employed to identify PDF inhibitor. The model of pharmacophore was valid according to the values of Area Under Curve of Receiver Operating Characteristic and GH-score. Using the validated model, 32 hit molecules were then retrieved from internal Indonesian medicinal plant database. Molecular docking was employed to identify the binding mode of each molecule to PDF active site, and top four molecules were subjected for MD simulation. All four molecules were stable along 50 MD run as indicated by RMSD values. Prediction of affinity employing MM-PBSA method implied that quercetin 3-(6"-malonylneohesperidoside) had a comparable affinity with that of BB2, which implied its potential as new PDF inhibitor.

5. REFERENCES

1. Lee, H.Y.; An, K.M.; Jung, J.; Koo, J.M.; Kim, J.G.; Yoon, J.M.; Lee, M.J.; Jang, H.; Lee, H.S.; Park, S.; Kang, J.H. Identification of Novel Aminopiperidine Derivatives for Antibacterial Activity against Gram-Positive Bacteria. *Bioorg Med Chem Lett* **2016**, *26*, 3148–3152, https://doi.org/10.1016/j.bmcl.2016.04.086.

2. Setzer, M.S.; Sharifi-Rad, J.; Setzer, N.W. The Search for Herbal Antibiotics: An In-Silico Investigation of Antibacterial Phytochemicals. *Antibiotics* **2016**, *5,* 30, https://doi.org/10.3390/antibiotics5030030.
3. Gao, J.; Liang, L.; Zhu, Y.; Qiu, S.; Wang, T.; Zhang, L. Ligand and Structure-Based Approaches for the Identification of Peptide Deformylase Inhibitors as Antibacterial Drugs. *Int J Mol Sci*. **2016**, *17*, 1141, https://doi.org/10.3390/ijms17071141.
4. Merzoug, A.; Chikhi, A.; Bensegueni, A.; Boucherit, H.; Okay, S. Virtual Screening Approach of Bacterial Peptide Deformylase Inhibitors Results in New Antibiotics. *Mol Inform* **2018**, *37*, 1700087, https://doi.org/10.1002/minf.201700087.
5. Spletstoser, J.T.; Dreabit, J.; Knox, A.N.; Benowitz, A.; Campobasso, N.; Ward, P.; Cui, G.; Lewandowski, T.; McCloskey, L.; Aubart, K.M. Discovery of Piperazic Acid Peptide Deformylase Inhibitors with in Vivo Activity for Respiratory Tract and Skin Infections. *Bioorg Med Chem Lett* **2019**, *29,* 2410–2414, https://doi.org/10.1016/j.bmcl.2019.05.028.
6. Shi, W.; Ma, H.; Duan, Y.; Aubart, K.; Fang, Y.; Zonis, R.; Yang, L.; Hu, W. Design, Synthesis and Antibacterial Activity of 3-Methylenepyrrolidine Formyl Hydroxyamino Derivatives as Novel Peptide Deformylase Inhibitors. *Bioorg Med Chem Lett* **2011**, *21*, 1060–1063, https://doi.org/10.1016/j.bmcl.2010.11.102.
7. Fieulaine, S.; Alves de Sousa, R.; Maigre, L.; Hamiche, K.; Alimi, M.; Bolla, J.-M.; Taleb, A.; Denis, A.; Pagès, J.-M.; Artaud, I.; Meinnel, T.; Giglione, C. A Unique Peptide Deformylase Platform to Rationally Design and Challenge Novel Active Compounds. *Sci Rep* **2016**, *6*, 35429, https://doi.org/10.1038/srep35429.
8. Lv, F.; Chen, C.; Tang, Y.; Wei, J.; Zhu, T.; Hu, W. New Peptide Deformylase Inhibitors Design, Synthesis and Pharmacokinetic Assessment. *Bioorg Med Chem Lett* **2016**, *26*, 3714–3718, https://doi.org/10.1016/j.bmcl.2016.05.077.
9. Hoover, J.; Lewandowski, T.; Straub, R.J.; Novick, S.J.; DeMarsh, P.; Aubart, K.; Rittenhouse, S.; Zalacain, M. Pharmacokinetics/Pharmacodynamics of Peptide Deformylase Inhibitor GSK1322322 against *Streptococcus pneumoniae*, *Haemophilus influenzae*, and *Staphylococcus aureus* in Rodent Models of Infection. *Antimicrob Agents Chemother* **2016**, *60*, 180LP–189, https://doi.org/10.1128/AAC.01842-15.
10. Guilloteau, J.P.; Mathieu, M.; Giglione, C.; Blanc, V.; Dupuy, A.; Chevrier, M.; Gil, P.; Famechon, A.; Meinnel, T.; Mikol, V. The Crystal Structures of Four Peptide Deformylases Bound to the Antibiotic Actinonin Reveal Two Distinct Types: A Platform for the Structure-Based Design of Antibacterial Agents. *J Mol Biol* **2002**, *320*, 951–962, https://doi.org/10.1016/S0022-2836(02)00549-1.
11. Wolber, G.; Langer, T. LigandScout: 3-D Pharmacophores Derived from Protein-Bound Ligands and Their Use as Virtual Screening Filters. *J Chem Inf Model* **2005**, *45*, 160–169, https://doi.org/10.1021/ci049885e.
12. Mysinger, M.M.; Carchia, M.; Irwin, J. J.; Shoichet, B.K. Directory of Useful Decoys, Enhanced (DUD-E): Better Ligands and Decoys for Better Benchmarking. *J Med Chem* **2012**, *55*, 6582–6594, https://doi.org/10.1021/jm300687e.
13. Li, H.; Leung, K.; Wong, M. Idock: A Multithreaded Virtual Screening Tool for Flexible Ligand Docking. In: *2012 IEEE Symposium on Computational Intelligence in Bioinformatics and Computational Biology (CIBCB)* 2012; pp 77–84, https://doi.org/10.1109/CIBCB.2012.6217214.
14. Morris, G.M.; Goodsell, D.S.; Halliday, R.S.; Huey, R.; Hart, W.E.; Belew, R.K.; Olson, A.J. Automated Docking Using a Lamarckian Genetic Algorithm and an Empirical Binding Free Energy Function. *J Comput Chem* **1998**, *19*, 1639–1662, https://doi.org/10.1002/(SICI)1096-987X(19981115)19:14<1639::AID-JCC10>3.0.CO;2-B.
15. Maier, J.A.; Martinez, C.; Kasavajhala, K.; Wickstrom, L.; Hauser, K.E.; Simmerling, C. Ff14SB: Improving the Accuracy of Protein Side Chain and Backbone Parameters from Ff99SB. *J Chem Theory Comput* **2015**, *11*, 3696-3713, https://doi.org/10.1021/acs.jctc.5b00255.
16. Wang, J.M.; Wolf, R.M.; Caldwell, J.W.; Kollman, P.A.; Case, D.A. Development and Testing of a General Amber Force Field. *J Comput Chem*, **2004**, *25*, 1157–1174, https://doi.org/10.1002/jcc.20035.
17. Jakalian, A.; Jack, D.B.; Bayly, C.I. Fast, Efficient Generation of High-Quality Atomic Charges. AM1-BCC Model: II. Parameterization and Validation. *J Comput Chem* **2002**, *23*, 1623–1641, https://doi.org/10.1002/jcc.10128.
18. Arba, M.; Nur-Hidayat, A.; Surantaadmaja, S.I.; Tjahjono, D.H. Pharmacophore-Based Virtual Screening for Identifying B5 Subunit Inhibitor of 20S Proteasome. *Comput Biol Chem* **2018**, *77*, 64–71, https://doi.org/10.1016/j.compbiolchem.2018.08.009.
19. Kollman, P.A.; Massova, I.; Reyes, C.; Kuhn, B.; Huo, S.; Chong, L.; Lee, M.; Lee, T.; Duan, Y.; Wang, W.; Dohini, O.; Cieplak. P.; Srinivasan, J.; Case, D.A.; Cheatham, T.E. Calculating Structures and Free Energies of Complex Molecules: Combining Molecular Mechanics and Continuum Models. *Acc Chem Res* **2000**, *33*, 889–897, https://doi.org/10.1021/ar000033j.
20. Arba, M.; Ruslin; Kalsum, W.U.; Alroem, A.; Muzakkar, M. Z.; Usman, I.; Tjahjono, D. H. QSAR, Molecular Docking and Dynamics Studies of Quinazoline Derivatives as Inhibitor of Phosphatidylinositol 3-Kinase. *J Appl Pharm Sci*, **2018**, *8*, 001-009, https://doi.org/10.7324/JAPS.2018.8501.
21. Arba, M.; Yamin; Ihsan, S.; Tjahjono, D.H. Computational Approach toward Targeting the Interaction of Porphyrin Derivatives with Bcl-2. *J Appl Pharm Sci* **2018**, *8*, 060-066, https://doi.org/10.7324/JAPS.2018.81208.
22. Miller, B.R.; McGee, T.D.; Swails, J.M.; Homeyer, N.; Gohlke, H.; Roitberg, A.E. MMPBSA.Py: An Efficient Program for End-State Free Energy Calculations. *J Chem Theory Comput* **2012**, *8*, 3314–3321, https://doi.org/10.1021/ct300418h.

6. ACKNOWLEDGEMENTS

MA acknowledge the Ministry of Research, Technology, and Higher Education, Republic of Indonesia, for funding this research.